ACTA MECHANICA SINICA (English Series), Vol.19, No.1, January 2002 ISSN 0567-7718
The Chinese Society of Theoretical and Applied Mechanics
Chinese Journal of Mechanics Press, Beijing, China
Allerton Press, INC., New York, U.S.A.

INVESTIGATION ON NONEQULIBRIUM RADIATION AND RELAXATION PHENOMENA IN SHOCK TUBES*

ZHU Naiyi (竺乃宜)† YANG Qiansuo (杨乾锁) ZHANG Hengli (张恒利)
YU Xilong (余西龙) HUANG Lishun (黄立舜)

(*Laboratory of High Temperature Gas Dynamics, Institute of Mechanics, Chinese Academy of Sciences, Beijing* 100080, *China*)

ABSTRACT: The experimental results for the excited time of the nonequlibrium radiation and the ionization behind strong shock waves are presented. Using an optical multichannel analyzer, InSb infrared detectors and near-free-molecular Langmuir probes, the infrared radiation, the electron density of air and the nonequlibrium radiation spectra at different moments of the relaxation process in nitrogen test gas behind normal shock waves were obtained, respectively, in hydrogen oxygen combustion driven shock tubes.

KEY WORDS: nonequlibrium radiation, relaxation phenomena, shock tube

1 INTRODUCTION

In order to learn more about the relaxation process in the flow around hypersonic vehicles, considerable attention has been paid to the effects of high temperature real gas[1~5]. In recent years, much effort has been devoted to numerically analyze this type of phenomena and the corresponding effects. However, not only the accuracy of such calculation is as yet to be verified, but also there are some physical parameters unknown for high temperature real gas. Because the excitation of the diatomic molecules resulting from shock front and the relaxation process of these molecules determine, to a large extent, the flow field and the radiation field around hypersonic reentry vehicles, the experimental research of the excitation and the relaxation of the molecules is quite important. The instantaneous translational temperature just behind strong shock waves is much higher than the equilibrium temperature. The process from the nonequilibrium state to the equilibrium state depends on the rates of vibrational relaxation, dissociation and ionization.

In this paper, we report the measurement results of the infrared radiation, the electron density of air and the nonequlibrium radiation spectra at different moments of the relaxation process in nitrogen test gas behind normal shock waves. A brief discussion on the experimental results is also given.

2 EXPERIMENTAL EQUIPMENT

In our experiment, one of the two shock tubes is 20 m in length and 800 mm in diameter, as shown in Fig.1. Its driver pressure is 3~8 MPa and the initial pressure in the test section can be set from 1.33 Pa to 133 Pa. The shock tube can provide shock waves with velocity in the range of 3~7 km/s ($Ma = 10 \sim 20$)[6]. Two ionization probes are used to detect the shock arrival to measure shock velocity, as well as for trigger of the optical multichannel analyzer (OMA). An InSb infrared detector in a radiometer and an oscillograph are used to record the radiation profile of the test gas behind the shock wave which passes through the Sapphire window. With a standard blackbody source and a mirror, the absolute radiation intensity of these gases can be detected.

Received 12 July 2001, revised 22 October 2001
* The project supported by the National Natural Science Foundation of China (19982005 and 10032050), and the National Defense Science Foundation of China (95JBA4.2ZK0402)
† E-mail: zny@imech.ac.cn

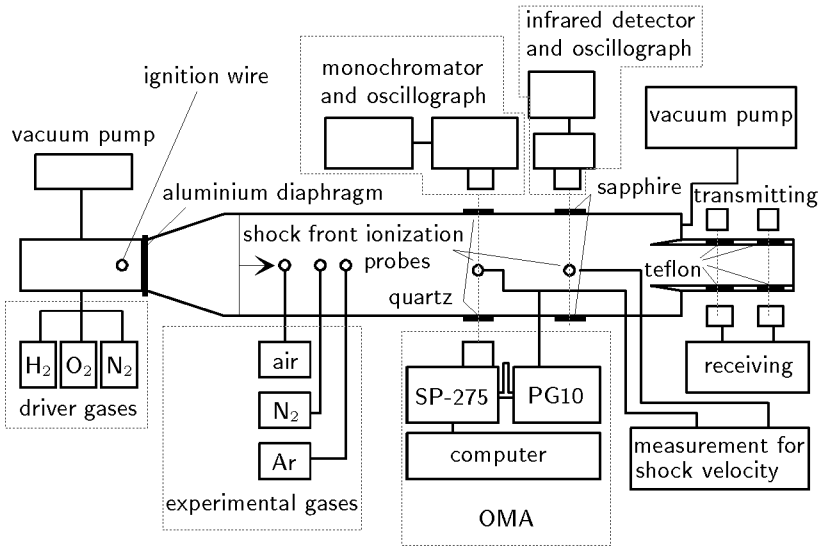

Fig.1 The experiment setup of ϕ 800 mm shock tube and the measurement instruments

Figure 2 shows the other shock tube of 78 mm in diameter and the measurement instruments for the radiation intensity profile, the shock velocity and the spectra. With an aluminium diaphragm of 2 mm thick, the shock tube can produce a stable shock wave with velocity of 6.4 km/s. The radiation profile and the signals from ionization probes 1 and 2 for shock velocity are recorded by a photo multiplier tube and a computer with a fast A/D converter. OMA is used to obtain the radiation spectrum at one moment. The initial pressure of oxygen, nitrogen and hydrogen in the driver section are 0.08 MPa, 0.08 MPa and 0.72 MPa, respectively. And the pressure of the driven section is firstly evacuated to 15 Pa by a vacuum pump and then increased to 100 Pa with the addition of nitrogen gas.

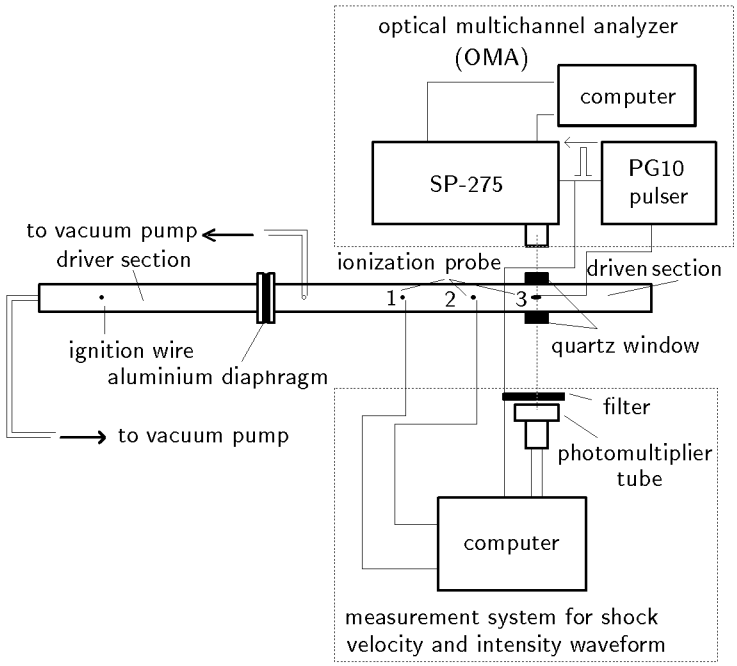

Fig.2 The experiment setup of Φ 78 mm shock tube and the measurement instruments

3 EXPERIMENTAL RESULTS

Figure 3 shows a typical infrared radiation profile of high temperature gas behind normal shock from ϕ800 mm shock tube where I_p is the peak of nonequilibrium radiation, I_e the value of equilibrium radiation and t_p the interval from the arrival of shock wave to the appearance of the nonequilibrium radiation peak. In addition, t_e is defined as the relaxation time of infrared nonequilibrium radiation of air, as shown in Fig.3.

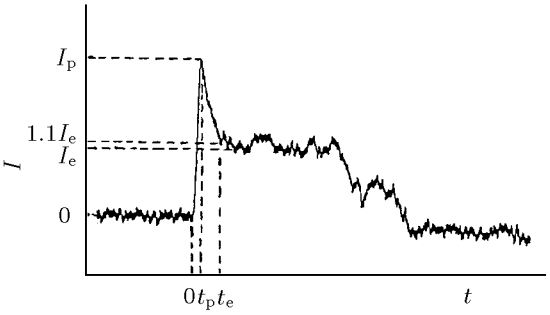

Fig.3 Infrared radiation profile of high temperature gas behind normal shock from ϕ800 mm shock tube

Using two InSb infrared detectors of wavelength of 1∼3 μm and 1∼5 μm, we record the radiation waveforms of the nonequilibrium state for the 2.7 μm first overtone band and the 5.3 μm fundamental band of NO in high temperature air behind a normal shock with different experimental parameters. And the ratios of the nonequilibrium radiation peak I_p to equilibrium radiation I_e are given in Table 1 where the unit of u_s is kilometer per second (km/s). It can be seen that the nonequilibrium radiation peak I_p is as high as 2∼7 times of equilibrium radiation I_e. With the same method, the excited time t_p and the relaxation time t_e of nonequlibrium infrared radiation with different parameters are also obtained. The experimental results are given in Table 2.

Table 1 The ratio of I_p to I_e

P_1= 80.0 Pa			P_1= 26.6 Pa			P_1= 12.0 Pa		
u_s	Ma	I_p/I_e	u_s	Ma	I_p/I_e	u_s	Ma	I_p/I_e
3.20	9.4	1.7	3.62	10.7	2.3	5.15	15.2	2.4
3.86	11.4	2.5	4.35	12.8	3.8	5.95	17.5	5.5
4.47	13.1	4.1	5.32	15.6	6.9			

Table 2 Excited time t_p and relaxation time t_e for different parameters

P_1= 80.0 Pa				P_1= 26.6 Pa				P_1= 12.0 Pa			
u_s	Ma	t_p	t_e	u_s	Ma	t_p	t_e	u_s	Ma	t_p	t_e
3.18	9.35	14.0	134.0	3.57	10.5	13.0	73.0	5.05	14.9	7.0	27.0
3.21	9.44	14.0	110.0	3.62	10.6	13.0	82.0	5.05	14.9	5.0	25.0
3.21	9.44	12.0	72.0	3.62	10.6	12.0	63.0	5.21	15.3	6.0	26.0
3.62	10.6	8.0	68.0	3.65	10.7	15.0	55.0	5.26	15.5	7.0	27.0
3.94	11.6	6.0	44.0	4.27	12.6	8.0	54.0	5.81	17.1	5.0	18.0
4.03	11.9	5.0	35.0	4.35	12.8	6.0	39.0	5.81	17.1	4.0	16.0
4.31	12.7	4.0	24.0	4.35	12.8	4.0	38.0	5.95	17.5	3.5	15.5
4.46	13.1	3.0	23.0	4.46	13.1	4.0	32.0	6.02	17.7	3.5	13.5
4.63	13.6	3.0	21.0	5.26	15.5	5.5	15.5				
				5.32	15.6	4.0	17.0				
				5.32	15.6	3.0	15.0				

The excited time t_p and the relaxation time t_e of infrared nonequilibrium radiation versus shock velocity at different initial pressure P_1 are plotted in Figs.4 and 5, respectively. It is clearly seen that the ratio I_p/I_e increases, as shown in Table 1, and the values of the excited time t_p and the relaxation time t_e multiplied by the initial pressure P_1 decrease, as revealed in Figs.4 and 5, with the rising of the shock velocity u_s.

The electron density behind normal shock waves and nonequilibrium ionization excited time t_{ep} from the arrival of shock front to the appearance of electron density peak have also been measured by near-free-molecular Langmuir probes. The structure of the Langmuir probe was described in Ref.[7]. Its receiving part of about 2 mm in length and 0.06 mm in diameter can provide a fairly high resolution in time and space. The experimental values of nonequilibrium ionization excited time t_{ep} behind normal shock at a series of Mach number are given in Table 3 and plotted in Fig.6.

For several sets of shock velocity and initial pressure, spontaneous emission spectra of air behind normal shock waves are acquired by OMA. From

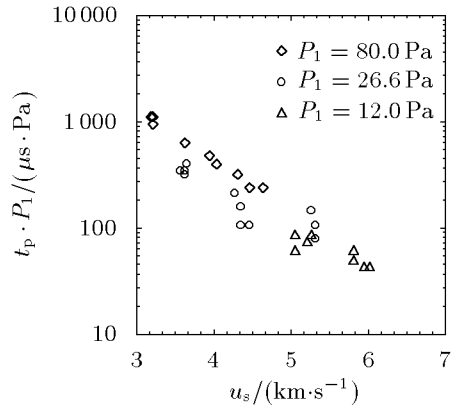

Fig.4 The infrared radiation excited times versus shock velocities

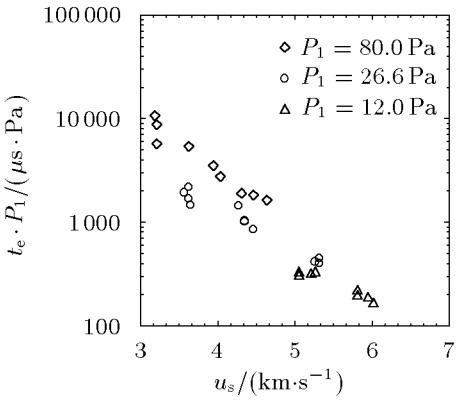

Fig.5 The relaxation time of infrared radiation versus shock velocities

Table 3 Shock velocity u_s and $t_\mathrm{ep} \cdot P_1$

$u_\mathrm{s}/(\mathrm{km} \cdot \mathrm{s}^{-1})$	Ma	$t_\mathrm{ep} \cdot P_1/(\mu\mathrm{s} \cdot \mathrm{Pa})$
4.59	13.5	70
4.86	14.3	70
4.93	14.5	100
5.10	15.0	42
5.20	15.3	44
5.58	16.4	26
5.78	17.0	34
6.15	18.1	17
6.26	18.4	17
6.32	18.6	17
6.46	19.0	13
6.77	19.9	12
7.48	22.0	9

these spectra, the intensity ratios at a certain wavelength in these spectra of nonequilibrium state and equilibrium state are computed, which are in agreement with the experimental results from the monochromator and photomultiplier tube.

We have also measured the intensity ratios at three wavelengths of 306.64 nm, 310.12 nm and 312.74 nm, where the first two locate at the (0,0) vibration band of OH $A^2\Sigma^+ - X^2\Pi$ and the third at (1,1) vibration band, in the experimental spectra of high temperature air behind the normal shock. Based on these ratios, the corresponding rotational and vibrational temperatures can be computed and the numerical results are given in Table 4. The equilibrium temperatures in Table 4 are calculated by ideal shock wave equations. It can be concluded that the rotational temperature quickly reaches its highest point, then declines to the equilibrium temperature, but the vibrational temperature directly rises to the equilibrium temperature according to the data in Table 4.

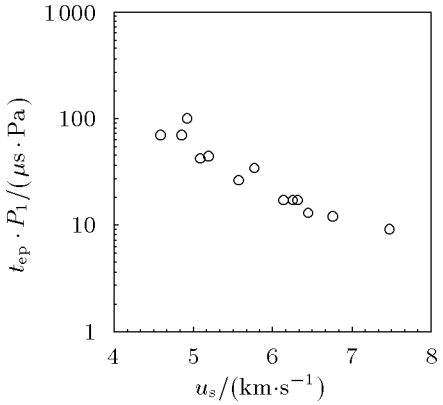

Fig.6 The ionization excited time versus shock velocities

Table 4 Rotational and vibrational temperatures based on OH spectra

(a) P_1=80.0 Pa, u_s=3.40 km/s, T_eq=3 320 K

Time/μs	T_r/K
0	4 600
80	3 400
164	3 480

(b) P_1=26.6 Pa, u_s=4.20 km/s, T_eq=4 380 K

Time/μs	T_r/K	T_v/K
−20	3 900	2 880
0	7 600	3 840
80	4 200	4400

(c) P_1=12.0 Pa, u_s=5.88 km/s, T_eq=5 560 K

Time/μs	T_r/K	T_v/K
−4	3 700	2 600
0	7 800	4 920
12	5 300	5 300

Using the experiment setup shown in Fig.2, the nonequilibrium spectra at up-side and down-side of the radiation profile are obtained, respectively. Figures 7(a′) and 7(b′) display the radiation profile and

the gate pulse of OMA and Figs.7(a) and 7(b) the corresponding spectra of the test gas at two moments for up-side. From Figs.7(a) and 7(b), it can be found that the nonequilibrium spectra at two moments are similar. The bands of $N_2^+(1-)(0,0)$, $N_2^+(1-)(1,1)$ and $N_2(2+)(0,2)$, clearly seen in the experimental results of Sharma and Gillespie[8], appear in our experimental spectra. Table 5 gives the peak ratios of the three bands of our experiment of a shock velocity 6.4 km/s and initial pressure 100 Pa and Sharma and Gillespie's experiment of a shock velocity 6.2 km/s and initial pressure 133 Pa. The work of obtaining vibrational and rotational temperature by comparing the computing spectrum with the experiment spectrum is under way.

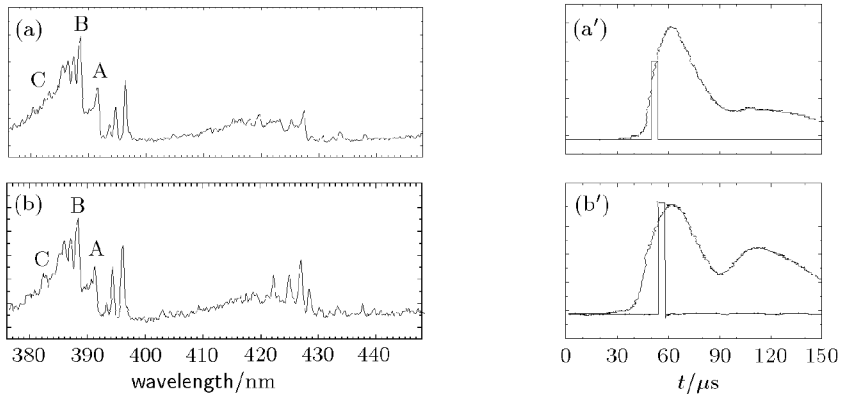

Fig.7 (a′) and (b′) the radiation profile of test gas and gate pulse; (a) and (b) the corresponding nonequilibrium spectrum. A, B and C indicate the three bands: $N_2^+(1-)(0,0)$, $N_2^+(1-)(1,1)$ and $N_2(2+)(0,2)$

Table 5 The peak ratios of three bands of $N_2^+(1-)(0,0)$, $N_2^+(1-)(1,1)$ and $N_2(2+)(0,2)$

	Peak ratios of $N_2^+(1-)(0,0)$, $N_2^+(1-)(1,1)$ and $N_2(2+)(0,2)$
Fig.7(a)	1:1.86:0.821
Fig.7(b)	1:1.79:0.882
Sharma et al.[3]	1:1.19:0.594

Another interesting phenomenon on nonequilibrium spectrum distribution is that the spectra at different moments of down-side are different from those of up-side, as shown in Figs.8(a), (b) and (c), although they share a similar feature. Several strong bands around 425 nm can be seen. The nonequilibrium spectra on down-side are obviously different from equilibrium spectra in previous experiments[8]. In fact, from Fig.7(b), the bands around 425 nm can be observed. The further research on nonequilibrium spectrum is continuing.

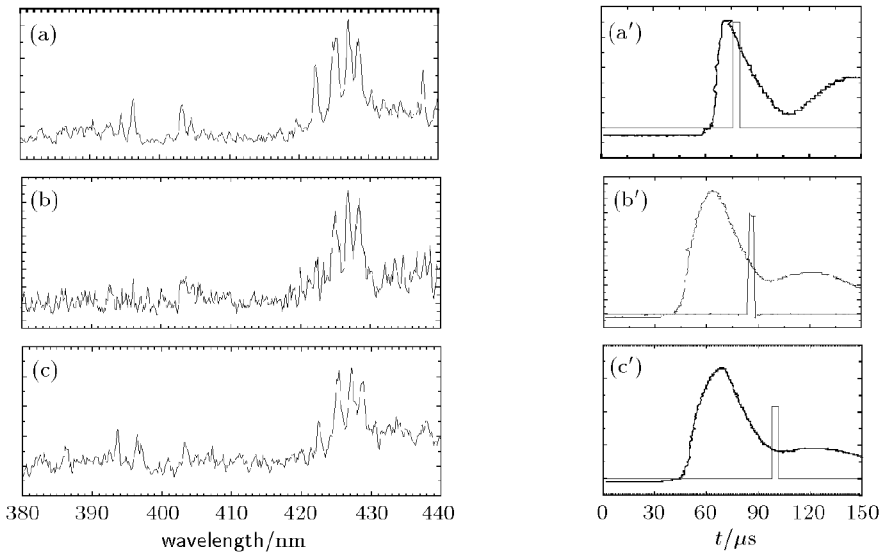

Fig.8 (a′), (b′) and (c′) the radiation profile of test gas and gate pulse; (a), (b) and (c) the corresponding nonequilibrium spectrum

4 CONCLUSIONS

The infrared nonequilibrium radiation peak I_p is as high as 2∼7 times of equilibrium radiation I_e in air behind normal shock waves with the initial pressure of 12.0∼80.0 Pa, the Mach numbers from 9.4 to 17.5. It is obvious that the ratio I_p/I_e increases, and the values of the excited time t_p and the relaxation time t_e multiplied by the initial pressure P_1 decrease, with the rising of the shock velocity U_s. The experimental values of nonequilibrium ionization excited time t_{ep} multiplied by the initial pressure P_1 decrease, with the rising of the shock velocity U_s (P_1 is 1.3∼133 Pa, U_s is 4.59∼7.48 km/s).

REFERENCES

1 Park C. Assessment of a two-temperature kinetic model for dissociating and weakly ionizing nitrogen. *J Thermophysics and Heat Transfer*, 1988, 2(1): 8∼16

2 Allen RA. Nonequilibrium shook front rotational, vibrational and electronic temperature measurements. *J Quant Spectrosc Radiat Transfer*, 1965, 5: 511∼523

3 Li HD. Experimental research on nonequilibrium radiative properties of high temperature gases in shook tube. *Acta Mechanica Sinica*, 1985, 17(2): 172∼176 (in Chinese)

4 Luo J, et al. Recent measurement of the near IR radiation from shock heated air. *Acta Mechanica Sinica*, 1984, 16(2): 185∼191 (in Chinese)

5 Sharma SP. Vibrational and rotational temperature measurements in a shock tube. In: Takayama K ed. Proc of 18th ISSW, Sendai, 1991-7-21∼26. Japan, Berlin: Springer Verlag, 1991. 683∼690

6 Zhu NY, Li HD, Zou HL, et al. Measurements of flow parameters in an 800 mm shock tube. *Acta Mechanica Sinica*, 1978, 10(3): 234∼237 (in Chinese)

7 Zhu NY, Li LX. A near-free-molecular Langmuir probe and the investigation of ionization shock structure. *Acta Mechanica Sinica*, Supplement, 1981, 13: 252∼258 (in Chinese)

8 Sharma SP, Gillespie W. Nonequilibrium and equilibrium shock front radiation measurements. *J Thermophysics and Heat Transfer*, 1991, 5(2): 257∼265